Review

Advanced Carbon Electrocatalysts for Selective Oxygen Reduction into Hydrogen Peroxide: Understandings of Active Sites

Jiaxin Su [1,2], Bingbing Xiao [1,2], Jun Wang [1,2],* and Xiaofeng Zhu [1,2],*

[1] State Key Laboratory of Environment-Friendly Energy Materials, School of Materials and Chemistry, Southwest University of Science and Technology, Mianyang 621010, China

[2] Tianfu Institute of Research and Innovation, Southwest University of Science and Technology, Chengdu 610299, China

* Correspondence: junwang091@163.com (J.W.); xfzhu@swust.edu.cn (X.Z.)

Abstract: Electrochemical conversion of oxygen-to-hydrogen peroxide (H_2O_2) through oxygen reduction (ORR) is becoming a green and effective solution to replacing conventional anthraquinone industry. Advanced carbon is currently one of the most promising catalysts for H_2O_2 electrosynthesis by a selective two-electron ORR (2e-ORR), owing to its chemical and catalytic merits. To realize better performance of 2e-ORR over advanced carbons, extensive efforts is devoted to constructing highly efficient carbon-based active sites, which requests in-depth understanding of their underlying catalytic roles. Here, an informative and critical review of recent investigations on active sites on advanced carbons for 2e-ORR is provided. Together with our recent findings, the review first highlights the promoting progress on heteroatom-doped carbons, and their direct/indirect contributions for 2e-ORR has been emphasized. Simultaneously, defect engineering of carbon scaffold is briefly demonstrated as a practical strategy for achieving outstanding H_2O_2 production. Meanwhile, the review also offers analysis on striking influence of surface modification for carbon active site. Finally, challenges and perspectives of the advanced carbon catalysts for 2e-ORR are outlined. Such reviewed fundamentals of active sites in this emerging field would shed light to future impactful progress in ORR and broader research of energy and catalysis.

Keywords: carbon-based materials; oxygen reduction reaction; H_2O_2 electro-synthesis; active sites; mechanism

1. Introduction

Hydrogen peroxide (H_2O_2) has been widely utilized in pulp bleaching, food/water disinfection and chemical fabrications. Upon the COVID-19 pandemic, the hygiene and sterilization capabilities of H_2O_2 has been further amplified, due to its environmental-friendliness and non-toxicity. The global market of H_2O_2 is currently estimated to be valued at more than $4 billion [1]. The market is projected to grow at a compound annual growth rate of about 5.7 percent from 2020 until 2028 [2]. Till now, more than 95% of H_2O_2 are produced via the energy-intensive anthraquinone process, which however produces organic contaminants and significant carbon dioxide emissions. Moreover, highly centralized anthraquinone industries are always criticized by their concentrated H_2O_2 (up to 70wt%) products. It not only leads to safety concerns in both storage and transportation sections, but also conflicts with end-users' needs of the dilute form [3–5]. Thus, it is of great economic and environmental importance to develop decentralized and green routes for H_2O_2 production.

To this end, recently, electrochemical synthesis of H_2O_2 is gaining tremendous interests from both academical and industrial sectors. Unlike conventional anthraquinone process, this emerging technology enables on-site production of H_2O_2 through either water oxidation reaction (WOR) at anodes or oxygen reduction reaction (ORR) at cathodes without any carbon footprints [6–8]. Nevertheless, compared with WOR, electrochemical ORR is recognized as a more facile and economic way to sustainably synthesize H_2O_2, owing to its lower overpotentials and higher selectivity [9]. In such process, oxygen molecules are reduced via a two-electron-two-proton ORR (2e-ORR) pathway, which inevitably completes with another four-electron-four-proton way (4e-ORR) [10,11]. Thermodynamically, the selectivity of ORR is mainly governed by the adsorption of intermediates (adsorbed O_2, OOH, O, OH, etc.), especially the OOH. Based on the *Sabatier principle*, the adsorption strength of the OOH should be just proper to enable rapid 2e-ORR, which is subject to physicochemical properties of electrocatalysts [12]. Thus, to achieve higher selectivity of 2e-ORR, researchers have developed a series of electrocatalysts to

acquire better selectivity of 2e-ORR, including functional carbons [13,14], noble metal compounds [15,16], metal chalcogenides [17–19] and single atomic catalysts [20,21]. Typically, an ideal ORR catalyst should be highly conductive and hierarchical porous to enable rapid mass and charge transfer [22,23]. Besides, practical H_2O_2 electrosynthesis requires economic benefits and chemical stability in both acid and alkaline media. In this regard, among the reported catalysts, carbon-based materials are considered as a promising substitution to expensive noble-metal benchmarks in electrochemical H_2O_2 synthesis, owing to their low-cost, abundant resource and chemical robustness [24–26].
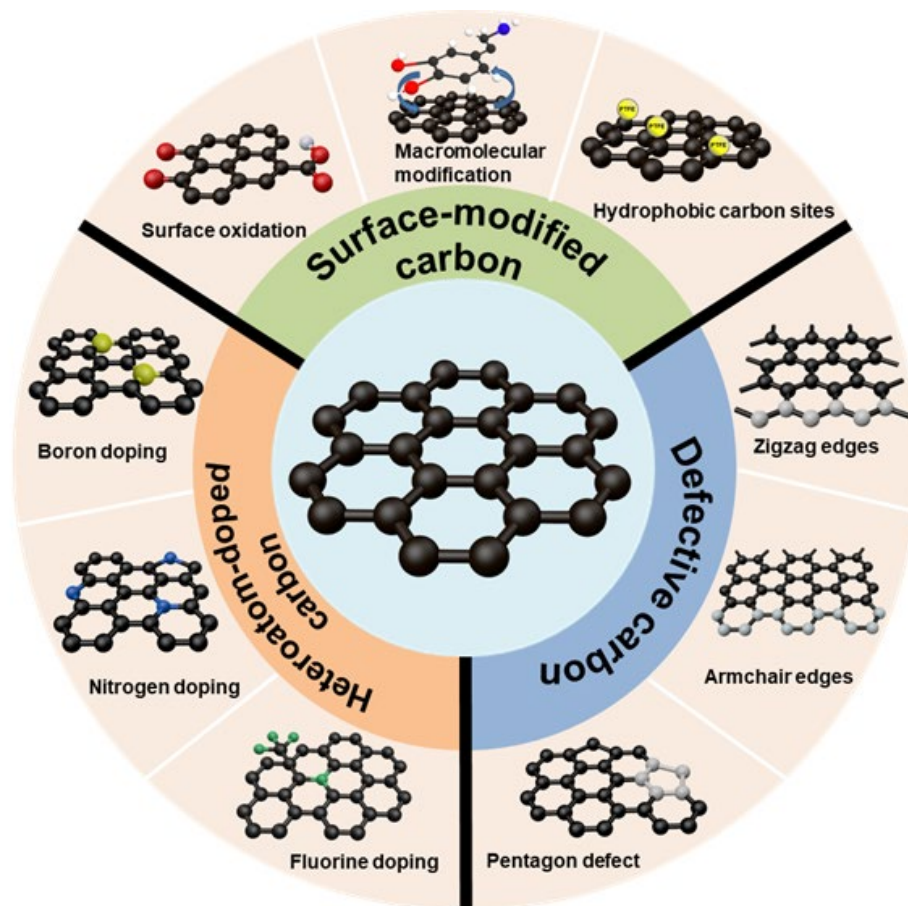

Figure 1. Advanced carbon-based electrocatalysts for 2e-ORR.

In view of promising industrial potential on carbon-based catalysts for H_2O_2 electrosynthesis, recent decade has seen a rapidly growing number of studies and publications in this field. Previous publications have comprehensively reviewed the recent progress in carbon-based catalysts for O_2-to-H_2O_2 conversion by focusing on the catalyst developments and their performance [1,24,27]. Besides, practical applications on H_2O_2 electrosynthesis, especially in environmental protection have also been previously reviewed [28]. However, to the best of our knowledge, a perspective overview on identification and mechanism of actual active sites in advanced carbons for electrochemical O_2-to-H_2O_2 has rarely been systematically and specifically reviewed. To address this gap, herein, a concise and critical review of recent advances in the metal-free advanced carbon catalysts for 2e-ORR is presented. Based on statistic summary on the actives and their 2e-ORR performance of the recent-reported carbons (Table 1), the review first briefly illustrates various advanced carbon electrocatalysts developed for 2e-ORR in Figure 1. Then, based on the types of heteroatoms, the nature and contributions of active sites in carbon materials, especially 2e-ORR mechanism of heteroatom doped carbons are highlighted, including electron redistribution, charge transfer and modified adsorption. The defect construction in carbon catalysts, such as edges and topological defects, is also discussed. Subsequently, as an emerging interest, surface modification as well as functionalization are specifically analyzed. Finally, current challenges and future perspectives of the advanced carbons for H_2O_2 electrosynthesis are outlined. This review aims to presenting a concise and in-depth analysis on carbon-based active sites for 2e-ORR and summarizing significant fundamentals in this emerging field. Through such a critical account, the understanding of carbon-based active sites and their reactive mechanism will be substantially deepened for 2e-ORR and broader energy conversions.

Table 1. Summary of carbon-based catalysts for H_2O_2 performance and the underlying mechanisms of the active sites.

Type	Catalyst	Active Sites	Electrolytes	2e-ORR Performance	Ref.
Heteroatom-doped carbon	P-NMG-X	Pyrrolic-N sites	0.1 M KOH	Yield: 30 mol $g^{-1}h^{-1}$ FE: 80%	[29]
	Biomass derived N/C	C defects and pyrrolic-N	0.1 M KOH	FE: 39.54% @ 0.6746 V_{RHE}	[30]
	Graphitic N-C	Graphitic-N	0.1 M KOH	Yield: 1286.9 mmol $g_{cat}^{-1}h^{-1}$; FE: 69.8%@0.1 V_{RHE}	[31]
	HPCS-S	Edge C-S sites	0.1 M KOH	Yield: 183.99 mmol $g_{Cat}^{-1}h^{-1}$;	[32]
	NF-Cs	Doped N and F atoms	0.1 M KOH	FE: 89.6%@0.74 V_{RHE}	[33]
	N-FLG	Pyrrole-N modified nearby C atoms	0.1 M KOH	Yield: 9.66 mol h^{-1} g_{cat}^{-1}	[34]
	CNT-U-15T	C atoms adjacent to Pyrrolic-N	0.1 M KOH	Selectivity: 93.5%	[35]
	B-doped rGO	Isolated B atoms	pH = 3.0, 6.5 and 10	Selectivity: 95–98.6% Yield: 95.63 mg cm^{-2} h^{-1}	[36]
	FS-CFs	F and S sites	0.1 M KOH	Onset: 0.814 @V_{RHE} Selectivity: 99.1%	[37]
	B-C	B heteroatoms	1 M KOH and 1 M Na_2SO_4	Selectivity: 85–90%	[38]
Defective carbon	MesoC,MicroC	pentagon defects	0.1 M KOH	Onset: 0.8V_{RHE}; Selectivity: >70%@0.7 V_{RHE}	[39]
	OCG	Defect C atoms adjacent to OFGs	0.1 M KOH	Yield: 473.9 mmol $g_{cat}^{-1}h^{-1}$; Selectivity: >70%@0.7 V_{RHE}	[40]
	PD/N-C	Pentagonal defects and N dopants	0.1 M $HClO_4$	Yield: 2923 mg L^{-1} h^{-1}	[41]
	S-D NC	S-C sites	0.1 M KOH	Onset: 0.78 V_{RHE} Selectivity: ~90%	[42]
	CB-Plasma	Edge active sites of O-defects	0.1 M KOH	FE: 100% Current: 300 A g^{-1}@0.6 V_{RHE}	[14]
	O-DG	Carbonyl on pentagon defect	0.1 M KOH	FE: 98.38%@0.55 V_{RHE}	[43]
	CF	Zigzag edge and zigzag pentagon sites	0.1 M KOH	Selectivity: >90%@0.6 V_{RHE}	[44]
	HCNFs	Edges and topological defects	0.1 M KOH	Selectivity: 97.3% Current: 220 A g^{-1}@0.65 V_{RHE}	[45]
	NBO-GQDs	B-atom site by the N atom and defect –OH	0.1 M KOH	Selectivity: >90% Yield: 709 mmol g_{cat}^{-1} h^{-1}	[46]
	MCNF	Edge defects	0.1 M KOH	Selectivity: >90% Current: 3 mA cm^{-2} @ 0.2 V_{RHE}	[47]
Surface-modified carbon	Edge-rich VG	Edge-bound ether-type groups	0.1 M KOH	Onset: 0.8 V_{RHE} FE: 100%	[48]
	F-mrGO	Ether and carbonyl groups	0.1 M KOH	Selectivity: ~100%	[49]
	O-CNTs	C atoms adjacent to OFGs (–COOH and C–O–C)	0.1 M KOH	FE: ~90% at 0.4–0.65 V_{RHE}	[50]
	GNP$_{C=O}$	Quinone functional groups	0.1 M KOH	Yield: 97.8 %@0.75 V_{RHE}	[51]
	CB600	O=C–OH and C–O–C groups	0.1 M Na_2SO_4	Yield: 517.7 ± 2.4 mg L^{-1}	[52]
	CB-PDA-A	Dipole-modified defective carbon	0.1 M KOH	Yield: 1.8 mol $g_{Cat}^{-1}h^{-1}$	[53]
	CTAB	Carbon sites (surfactants modified)	0.1 M KOH	Selectivity: 95.2%	[54]

PTFE/CB	Hydrophobic carbon sites	0.05 M Na_2SO_4	Yield: 101.67 mg h^{-1} cm^{-2}	[55]
Na$^+$/CB	Carbon sites at Na$^+$ modulated surface	0.1 M H_2SO_4	Selectivity: over 80%	[56]
CB-PTFE	Carbon sites at hydrophobic interfaces	0.05 M Na_2SO_4	Selectivity: >97%	[57]

2. Influence of Heteroatom Dopants on Carbon Active Sites

Perfect carbon framework is generally considered inactive towards electrocatalytic reactions, due to its homogeneous π electronic structure [58]. Thus, to create carbon active sites, one of the commonly used strategies is doping heteroatoms into carbon matrix, such as nitrogen (N), boron (B), fluorine (F), oxygen (O), phosphorus (P), and sulfur (S). By virtue of their varied electronegativities, electronic asymmetry could be deliberately introduced, thereby forming active sites for electrochemical ORR.

Among the heteroatom-doped carbon catalysts, N-doped carbon has been the most extensively investigated, recently. Despite of the three major types (i.e., pyridinic, graphitic and pyrrolic N), it is generally believed that N dopants could alter electronic structure of nearby carbon atoms, making them active sites for ORR [59,60]. Such modifications are basically attributed to the high electronegativity of N atoms compared to C atoms, thus inducing positive charges on neighboring C atoms [61,62]. However, charged carbon active sites might deliver considerable faradaic currents for ORR, while the selectivity of 2e-pathway is not necessarily ensured. In fact, the ORR selectivity of the N-doped carbons is largely depended on the types of N dopants. Among the three main N dopants, pyridine-N has been commonly recognized to render preferential 4e-ORR in basic electrolytes [63–66]. In this case, pyridine-N could either confer relatively high positive charged π-orbitals on α-C atoms [61,67] or transfer rich free lone-paired electrons to antibonding orbitals of O_2 reactants [34,68], thus leading to the cleavage of O–O bonds and over-reduction of *OOH intermediates. Interestingly, on the contrary, Daniel and co-workers found that the pyridine-N could enable effective formation of H_2O_2 under acidic conditions [69]. To note, the protonation of pyridine-N would lead to a weaker combination with OOH intermediates and thus help to maintain O–O bonds in acidic environment. Similarly, Sun et al. have developed N-doped porous carbon through pyrolysis of ordered mesoporous carbon with polyethyleneimine [70]. H_2O_2 selectivity of 95.3 % was achieved over the prepared N-doped carbons in 0.05 mol L^{-1} H_2SO_4 solution, while a considerable H_2O_2 production rate of 570.1 mmol g$_{cat}^{-1}$ h^{-1} was observed in neutral solution. X-ray photoemission spectroscopy (XPS) analyzed the changes of different N content before and after ORR, revealing that pyridine-N and graphite-N was more catalytically active in both acidic and neutral/basic ORR process, respectively (Figure 2a).

The contributions of graphite-N towards 2e-ORR were also reported in some studies. For instance, Rao et al. observed two ORR peaks in doped carbon catalyst with higher graphitic-N content, standing for 2e-ORR into H_2O_2 and subsequent reduction to H_2O, respectively [71]. Similar to pyridinic-N, the intrinsic capability of 2e-ORR over graphite-N was mainly assigned to the slightly positive charged carbon atoms around graphite-N [72–74]. These C atoms would act as Lewis acidic sites and suppress the adsorption of ORR intermediates. Likewise, Zhang et al. proposed an appealing mechanism of 2e-ORR on graphitic-N sites [31]. 2e-ORR was firstly initiated by proton-coupled electron transfer, and the graphite-N can induce charge redistribution by providing a single electron to the p–π conjugated system. Consequently, the adsorption of oxygen on neighboring α-C atoms could be enhanced, boosting the conversion into the *OOH intermediate (Figure 2b). And then, charge re-equilibrium of graphite-N would facilitate the desorption of *OOH, yielding high H_2O_2 selectivity (up to 75%) on such graphitic-N sites in alkaline electrolytes. On the other hand, pyrrole-N has been widely reported as active sites for 2e-ORR. Qiao and collaborators introduced a porous N-rich few-layered graphene (N-FLG) with tunable pyrrole-N content [34]. Experimental results identified a close correlation between the content of pyrrole-N and the 2e-ORR selectivity, reaching around 95% conversion of O_2-to-H_2O_2 over N-FLG-8 (Figure 2c). The excellent 2e-ORR performance was assigned to the electronically modified nearby C atoms, which optimized the absorption of OOH species over the heterocyclic distorted sites. Moreover, Wan et al. successfully prepared N-doped single-walled carbon nanotubes (CNT-U-15T) by a microwave-assisted pulsed heating method [35]. It was discovered that the pyrrole-N moieties could donate two p-electrons to the π-conjugated system in the carbon configuration, which might extensively adjust the electron density of nearby C atoms. As a result, the ORR process over the pyrrole-N-doped CNT-U-15T was simulated to possess ideal electron transfer numbers (~2) for the peroxides formation within a wide range of potentials (0.30–0.65 V$_{RHE}$), proving its excellence in 2e-ORR.

It can be seen that heteroatoms with higher electronegativity can interfere with the electroneutrality of the carbon system and promote charge redistribution, which could be beneficial to the generation of H_2O_2 [60,75,76]. Bearing this thought, Zhao et al. modulated the electronic structure of porous carbon by doping F with even higher

electronegativity compared to N [77]. With 3.41 at.% of F atoms, the F-doped carbons exhibited exceptional H_2O_2 selectivity of 83.0%–97.5%, producing a peroxide generation rate of 112.6–792.6 mmol $g^{-1}h^{-1}$. To further elucidate the underlying effects of F dopants, three different models were constructed (Gr-F, Gr-F_2, and Gr-F_3) by theoretical calculations. Simulations revealed that F doping resulted in a weaker adsorption energy for O_2 molecules compared to the F-free counterpart, facilitating the activation of O_2 molecules on the carbon planes. Among these models, Gr-F_2 sites presented a weaker OOH-binding energy, promoting the generation of H_2O_2. Meanwhile, the formation of C-F covalent bonds in F-modified CNT could lead to local structural deformation of carbon. The resulting CNT-F-0.6 showed a high electrical H_2O_2 production concentration and current efficiency of 47.6 mg L^{-1} and 89.4%, respectively. The high 2e-ORR performance was attributed to the formation of C-F on the surface of the CNT by F, and the weak binding energy of the C-F with OOH promoted the 2e-ORR [78].

Contradicting to F and N atoms, B dopants with less electronegative than C normally produce negative charges in local carbon matrix, which make itself favoring for the adsorption and reduction of oxygen molecules [38,79,80]. Xia et al. demonstrated that B-doped carbon materials could exhibit very low overpotentials for 2e-ORR by Density Functional Theory (DFT) calculations and experimental results [38]. However, like N-dope cases, the ORR selectivity of the B-doped carbon catalysts was majorly governed by the specific doping patterns [81]. To figure out their critical roles in 2e-ORR, Chol Ri et al. prepared different B-doped rGO catalysts and found that the 2e-ORR selectivity of B-doped rGO was related to the B content and oxygen transfer conditions [36]. The interconnected B atoms, in their case, served as centers for 4e-ORR, while isolated B atoms acted as the active sites for 2e-ORR in B-doped rGO. Therefore, after proper optimization of isolated B concentrations, the synthesized catalysts exhibited high 2e-ORR selectivity in the range of 95–98.6%, with H_2O_2 yields as high as 95.63 mg cm^{-2} h^{-1} at the current density of 200 mA cm^{-2}. To establish a systematic comparison of heteroatom doping on the performance of 2e-ORR, Wang et al. fabricated B-, N-, P- and S-doped carbon nanomaterials, and B-doped C catalyst presented the best 2e-ORR activity with high H_2O_2 selectivity (85–90%) under alkaline condition (Figure 2d) [38]. Unlike N and F dopants, B heteroatoms *per se* could serve as active sites for 2e-ORR, rather than neighboring C atoms. Further, B dopant sites offered the best *OOH adsorption energy, thereby lowering thermodynamic barriers for 2e-ORR.

Although being elements of the same main group with N, the catalytic activity of P-doped carbon catalysts for the electrochemical generation of H_2O_2 has been less studied. Among the limited work, Liu et al. synthesized P-doped macroporous/mesoporous/microporous carbon (P-MC) electrocatalysts, which exhibited excellent FE of more than 98% under alkaline conditions. The significant enhancement of the catalytic activity of the P-MC was attributed to the different electronegativity between the P and C atoms, which redistributed the electrons of the carbon [82]. However, the situation is different for S-doping, which induces charges and increases the spin density of carbon, resulting in lower overpotentials for 2e-ORR. For instance, Chen et al. used a silica template method to prepare C and S composites. 2–5 nm sulfur nanocrystals were confined within hollow porous carbon spheres, and the interfacial electron distribution was altered, effectively facilitating electron transport and leading to high 2e-ORR activity and selectivity. DFT showed that the appearance of C-S edge sites greatly reduced the overpotential, which significantly improved the electrocatalytic performance [32].
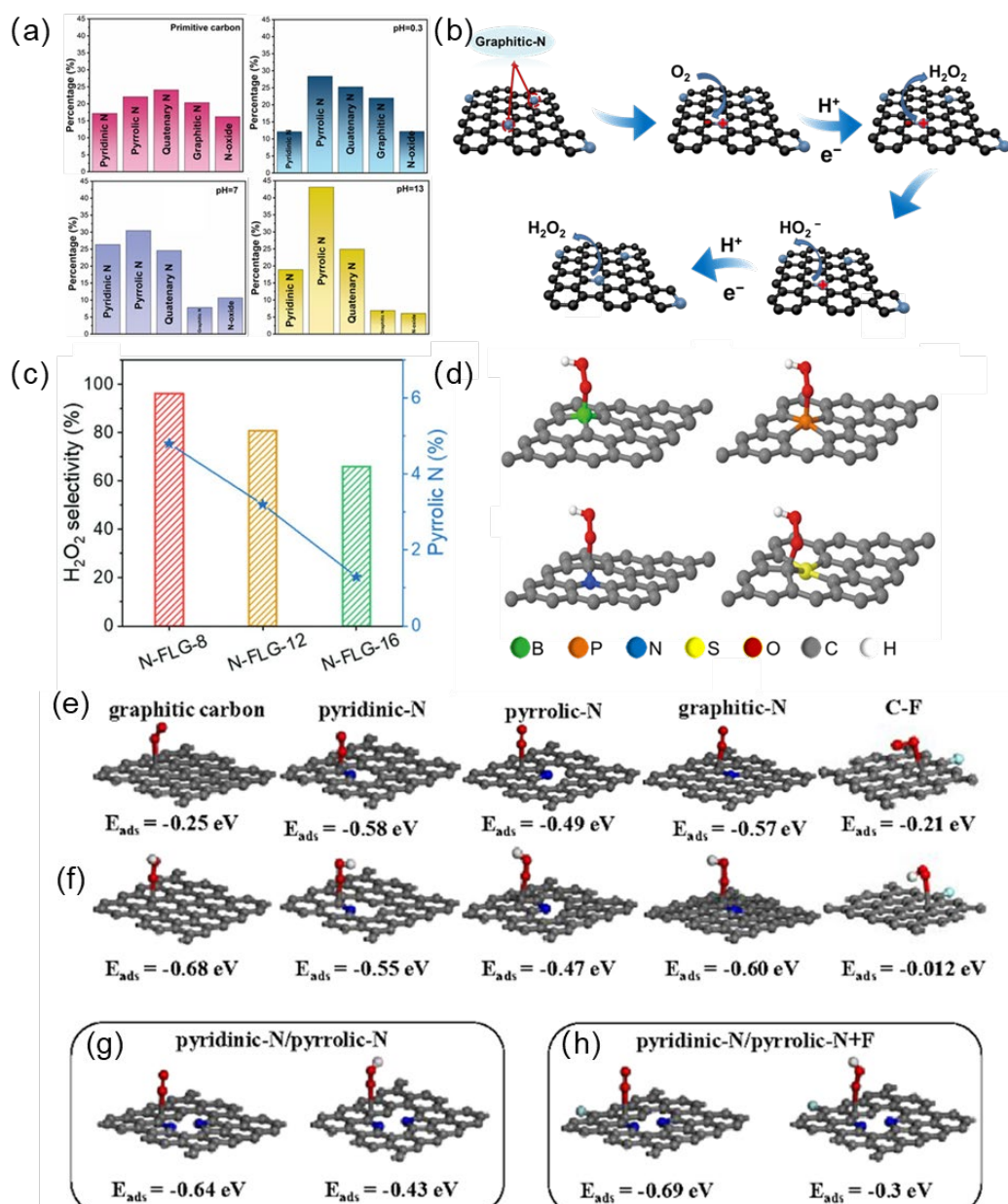
Figure 2. (**a**) The relative content of nitrogen in nitrogen-doped porous carbon before and after catalysis under acid, neutral and basic conditions, Data from Ref. [70]. (**b**) The mechanism diagram of 2e-ORR on graphite-N-doped carbon catalysts. Original reproduced and concept from Ref. [31]. (**c**) Relationship between H_2O_2 selectivity and the content of pyrrolic-N [34]. (**d**) Preferred *OOH adsorption configurations on B-, P-, N-, and S-doped graphene, respectively [38]. (**e**) The optimized O_2 adsorption energy and the doping structure. (**f**) The optimized *OOH adsorption energy and the doping structure. (**g**) and (**h**) The optimized O_2 and *OOH adsorption energy and the doping structure on the various N species [33].

To pursue better 2e-ORR performance, the synergistic effect between different doped atoms has also been considered, thus multi-doped carbons have been consequently developed. Doping of two or more heteroatoms would substantially increase the population of active sites, thus resulting in better activity for 2e-ORR. For example, in N and F co-doped carbon hollow nanospheres (Figure 2e–h), N and F dopants were responsible for ORR activity and 2e-selectivity, respectively, synergistically leading to the highly efficient carbon-based electrocatalysts for H_2O_2 production [33]. In addition, F dopants could enhance the interaction between the active sites and oxygen, thereby improving the production of H_2O_2. In this regard, Gu et al. prepared a series of O or F mono- and O/F co-doped CNTs with different O/F ratios for 2e-ORR [83]. By incorporating the COOH and C-F species, the electronic structure of carbon atoms was disrupted and influenced by a strong electropositive effect, which was favorable for the end-on adsorption of O_2 molecules (Pauling model) and then 2e-ORR. Furthermore, compared with the mono-doped F material, the addition of S could also generate an internal electric field at the S-C interfaces [84,85], leading to enriched electron population over the carbon atoms and accelerated electron transportation [76,86]. Thus,

Xiang et al. investigated the 2e-ORR performance of samples with different S and F doping [37]. Among them, F/S dual-doped metal-free carbon fiber catalyst exhibited the best 2e-ORR performance with an onset potential of 0.814 V_{RHE} and a state-of-the-art H_2O_2 selectivity of 99.1%. It was demonstrated that enhanced intermolecular charge transfer and electron spin redistribution generated by F and S sites incurred the optimized adsorption strength of the *OOH intermediate towards 2e-ORR.

In general, heteroatom doping strategy is basically breaking the electroneutrality of perfect carbon, owing to the distinct electronegativity of the dopants. Thus, these created charged sites, either dopants (B and P doping) or nearby C atoms (F and N doping), could adjust the adsorption of OOH intermediates to harvest decent 2e-ORR selectivity, and the reactivity of the doped carbon materials is more related to the dopants (type and content of dopant atoms). Compared with mono-doping, co-doping could introduce a different heteroatom into carbon platform, synergistically affecting with another dopants. Unlike mono-doping, the selection and combination of the heteroatoms rather than the electronic negativity would be the decisive factor in electrocatalytic activity in this configuration. Also, doping locations in the carbon matrix strongly determine the active sites and their corresponding roles, which implies abundant scientific opportunities in precise controlling of heteroatom doping.

3. Carbon Defects as Active Sites for 2e-ORR

Heteroatom doping can indeed regulate the electronic configurations of carbon framework, while over-doping may also jeopardize the electroconductivity by lowering the degree of graphitization [87,88]. It inevitably leads to the decrease of the electrochemical performance, and thereby defect engineering without involving any heteroatoms has been explored. Carbon materials with various types of defects can geometrically create active sites for 2e-ORR. Plus, electrical asymmetry would also be introduced by breaking hexagonal ring of the aromatic carbon network. Nevertheless, the inherent defect density in pristine carbon is too low to generate enough catalytic capacity, therefore requiring further defect construction to induce textual distortions and charge reconfiguration in the carbon material [89,90].

The reactive carbon defects mainly include edge and topological defects. Recent decades have witnessed increasing scientific attentions over edge site-rich carbons, because of their outstanding superiority to planar-rich counterparts for electrochemical applications [11]. Notably, as often the case, oxygen would be bonded with carbon defects to compensate the exposed unsaturated coordination in both zigzag and armchair edges. For instance, Bao et al. exfoliated graphite by ball milling to form defective graphene, resulting in a superior ORR activity [91]. Simulations combined with XPS analysis spotted that the zigzag edges occupied by –C=O and C–O–C rather than armchair edges accounted for the improved ORR performance, and the C atoms adjacent to these two functional groups were identified as active sites. At the same time, Roman et al. developed a graphene-based nanomaterial catalyst, showing 94±2% H_2O_2 selectivity and an onset potential of ~0.79 V_{RHE} in alkaline environment [92]. In contrast, their results showed that both the armchair and zigzag edges saturated by either the carbonyl (C=O) or the hydroxyl (C–OH) groups can significantly change the local electronic structure of C active sites, thus favoring selective 2e-ORR and effective H_2O_2 generation. Despite of the above debates, many studies ignored such discrepancy and purposely increase the defect concentrations in the carbon skeleton, in order to produce abundant exposed active sites. Sa and colleagues, for instance, prepared a two-dimensional graphitized carbon catalyst with a large amount of edge defects, achieving sustainable production of H_2O_2 for 16 h with faradaic efficiency reaching almost 99% [11]. The linear relationship between defect content and 2e-ORR performance further disclosed the active nature of carbon sites at defects. Likewise, the fabrication of nano-sized pores on the basal plane can also generate additional carbon edges. The pore structure allows the carbon edges to be fully exposed to the reaction substrate and electrolyte, facilitating oxygen diffusion mass transfer. As shown in Figure 3a,b, Jing and coworkers employed an organic-inorganic hybrid co-assembly strategy prepare mesoporous carbon fibers (MCNFs) with controllable edge densities [47]. The as-prepared MCNFs exhibited cathodic current density of up to 3 mA cm^{-2} (@ 0.2 V_{RHE}) and a selectivity of >90% for H_2O_2. Apart from the accelerated mass transfer, suitable binding energy of the *OOH at the defect edge sites also improved the electrocatalytic activity and selectivity towards H_2O_2, as evidenced by their spectroscopical and DFT results.
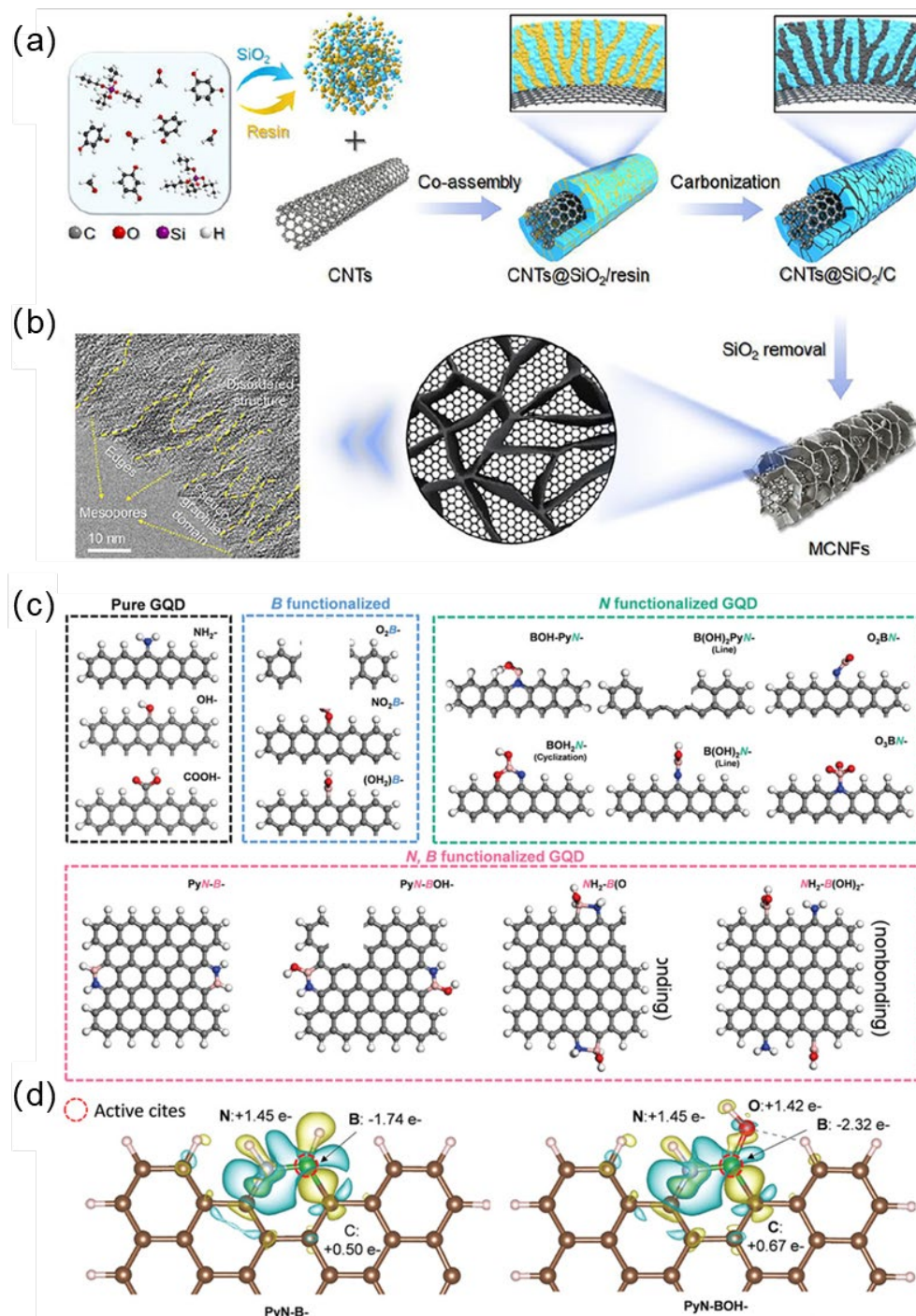
Figure 3. (**a**) Schematic illustration of the preparation of MCNFs. (**b**) Corresponding HRTEM images [47]. (**c**) The possible models of B, N, O modified GQDs. (**d**) Charge density difference mapping images of proposed doping structures (Top view). Charge accumulation: yellow; Charge depletion: cyan [46].

Meanwhile, another way to constructing edge sites is downsizing carbon nanomaterials. Graphene quantum dots (GQDs), as unique zero-dimensional carbon materials, contain abundant edge sites [93]. Such nano-scaled edge sites tend to be coordinated with functional groups and heteroatoms, inducing desirable catalytic activity [94]. As a prediction, Fan et al. screened N and B active site configurations over GQDs carbon model through DFT theoretical simulations, forming N-B-OH sites (NBO-GQDs) [46]. Consequently, NBO-GQDs was theoretically able to present overwhelming 2e-ORR performance. Experimental evidence also confirmed their simulation results. The resulting NBO-GQDs illustrated a high selectivity of H_2O_2 of over 90% and the mass activity of 709 mmol $g_{catal}^{-1} h^{-1}$ in the flow cell. They proposed that the synergistic modulation of the B-atom site by the N atom and defect-OH weakened the adsorption of the OOH* at the active site, leading to a highly selective of H_2O_2 performance (Figure 3c,d).

Unlike the edges, structural defects within the basal carbon planes mainly induce asymmetric local electron redistribution to tune the electrocatalytic capability of carbon materials [39,95]. In particular, the topological pentagonal defects with one carbon vacancy could form larger local charges than hexagonal defects, due to structural distortion [96]. Lee et al. investigated the electronic properties of various topological defects in carbon nanotubes. They found that the electronic state of pentagonal sites was close to the valence band, which could serve as electron acceptors, whereas that of the heptagonal sites approached the conduction bands, working as electron donors [97]. Both of them could successfully generate enough charge asymmetry over carbon framework, which then facilitated H_2O_2 synthesis via 2e-ORR.

However, carbon materials with individual defects are still far inferior to noble metal-based compounds in ORR, due to co-presence of different defects. In view of these, recent studies have endeavored to orientate the construction of specified defective species, with accurate identification of their location and density. Bao et al. pioneeringly synthesized two porous carbon materials with microporous (MicroC) and mesoporous carbon (MesoC) for H_2O_2 synthesis via 2e-ORR. Electrochemical results pictured that the prepared carbon nanotubes achieved high H_2O_2 selectivity over 70% and excellent onset potential (0.7 V_{RHE}), approaching ideal thermodynamic equilibrium. As revealed by DFT (Figure 4a,b), the pentagon defects located at both the MicroC and MesoC acted as active sits in 2e-ORR process, by tailoring the electronic structure of carbon atoms [39].
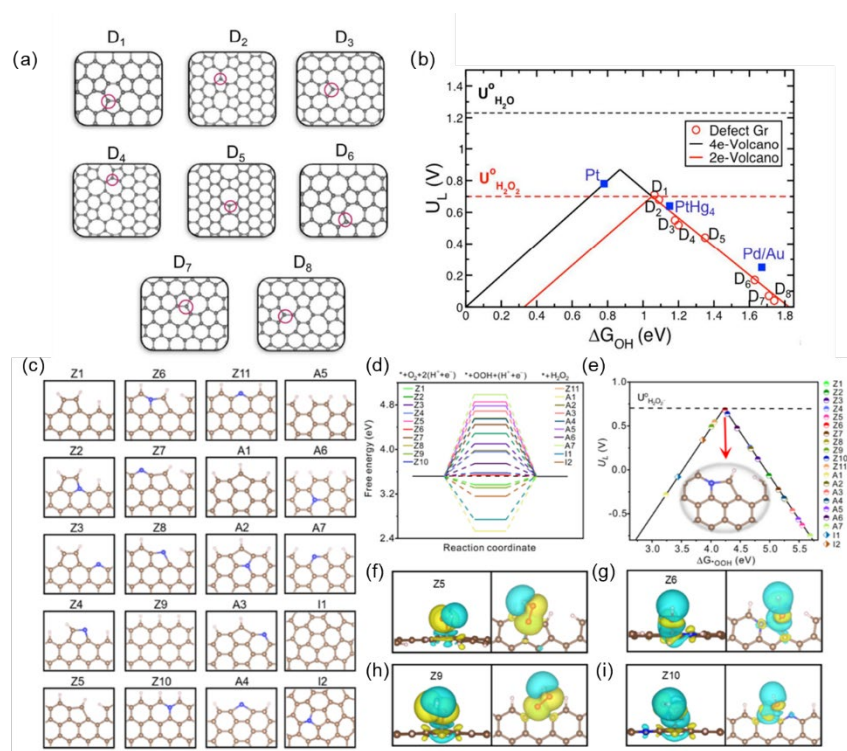

Figure 4. (**a**) Different defect type configurations examined of the two porous carbon materials. (**b**) Volcano plot of 2e-ORR (red) and 4e-ORR (black) [39]. (**c**) DFT results of different atomic models. (**d**) Standard free energy diagram of the types of N dopants for 2e-ORR. (**e**) Volcano plot between U_L and ΔG_{*OOH} for 2e-ORR. (**f**) The charge density of non-doped pentagon defect, (**g**) Gr-N doped pentagon defect, (**h**) non-doped graphene edge, and (**i**) Gr-N doped graphene edge before and after interacting with *OOH; The positive charge: yellow; The negative charge: cyan [41].

Moreover, Zhang et al. creatively adopted pentagonal-defects engineering on N-doped carbon nanomaterials (PD/N-C), using fullerene as a precursor with ammonia treatments [41]. The PD/N-C catalyst achieved a faraday efficiency (FE) of nearly 100% and a high H_2O_2 yield of 2923 mg L^{-1} h^{-1} under acidic condition. Experimental and theoretical results indicated that the pentagonal defects facilitate electron transport from the carbon substrate of the adjacent N-C sites to the adsorbed *OOH. Consequently, the synergistic interactions between the pentagonal defects and N doping significantly influenced and modulated the geometrical and electronic structure of the nanocarbon, leading to optimized *OOH adsorption strength and facilitating H_2O_2 production (Figure 4c–i). Similarly, continues from the previous work, Lu et al. then reported 2e-ORR enhancement that could be achieved by directionally settling the intrinsic carbon defects next to the S dopants [42]. Their work was devoted to the construction of topological carbon defects in the presence of S in which S-doped defective nanocarbon (S-DNC)

was synthesized by direct pyrolysis of fullerenes. Such S-DNC exhibited an exceptional ORR onset potential of 0.78 V_{RHE} and high selectivity (~90%) for the 2e-ORR. DFT calculations showed that synergistic interactions between S heteroatoms and pentagonal defects promoted charge redistribution in the carbon substrate. As a result, the electron density on the S-adjacent atoms (i.e., the active centers were located at the S-C sites) was increased, which optimized the adsorption energy of the ORR intermediates and consequently decreased the total energy barrier of the ORR. These studies fully demonstrated the spacious potential of combining topological pentagonal defects and heteroatom dopants to realize the 2e-ORR performance of the catalysts.

4. Interfacial Effects on Carbon Active Sites

Both doping and defect engineering introduce electronic asymmetry by breaking carbon matrix, while recent endeavors focus on surface modifications, leaving carbon framework intact. The efforts and implementations have been mainly concentrated on planting functional groups, short/long chains, and polymer molecules onto carbon interfaces [98,99]. Thus, the intermediates adsorption would be tuned and 2e-ORR can be boosted via their thermodynamic and kinetic advantages. Among them, oxygen functional groups (OFGs) have been widely reported for their unique capability in reinforcing 2e-ORR selectivity of carbon catalysts. Such OFGs could either perform as active sites or modulate the electronic structure of neighboring C atoms [100], thus the activity and selectivity for 2e-ORR over carbon-based catalysts could be further modified [101–103]. The interaction and prompting roles of OFGs are believed to be governed by the particular properties of various carbons and OFGs, leading to different explanations for the mechanism in 2e-ORR process.

Among the first attempts, Cui et al. pioneered and developed an oxidized carbon nanotubes (O-CNTs) by treating CNTs with concentrated nitric acid [50]. Compared with pristine CNTs, O-CNTs exhibited lower overpotentials (~130 mV) and higher H_2O_2 selectivity (~90% at 0.4–0.65 V_{RHE}) in alkaline solution. Given that the positive correlation between the O content and their activity and selectivity for 2e-ORR, the C atoms adjacent to OFGs (–COOH and C–O–C) were revealed to be active sites for 2e-ORR, as indicated by DFT calculations. Unlike oxidation routes, OFGs-carbon could also be prepared via a partial reduction of graphene oxide (F-mrGO) [49]. Under alkaline conditions, the F-mrGO catalysts with high concentrated cyclic ether groups could produce H_2O_2 at nearly 100% H_2O_2 selectivity and excellent stability (over 15 h). As unveiled by near-edge X-ray absorption fine structure (NEXAFS) and *in-situ* Raman, the sp^2 hybridized C near-ring ether defects that generated by OFGs was the active site for H_2O_2 electro-generation.

On the other hand, some research has also argued the direct participation of OFGs in 2e-ORR process, where OFGs instead of C atoms were regarded as active sits. Han and co-workers constructed targeted quinone groups onto carbon materials with overhanging edge sites, and the resulting catalysts yielded H_2O_2 at an efficacy of 97.8% [51]. By adjusting the quinone content of the carbon catalyst from 4.5% to 7.4%, the ring current (standing for H_2O_2 formation) was correspondingly increased during rotating ring disk electrode (RRDE) measurements, confirming that the quinone species were the active sites for the 2e-ORR (Figure 5a). Furthermore, the effect of the position of quinone groups on the 2e-ORR was investigated by DFT, demonstrating that the quinone functional groups on the carbon edges delivered the highest 2e-ORR activity (Figure 5b,c). Meanwhile, to gain insights into the reaction mechanism, Xie et al. also systematically investigated the activity of various active sites in O-doped carbon materials, based on the DFT calculations [104]. Among these simultaneous generated OFGs during the oxidation of carbon surface, ether and carbonyl groups were identified as the sources of high 2e-ORR activity. Furthermore, a significant synergistic effect between different OFGs was also spotted, when the doped OFGs are combined with specific oxygen structures, especially epoxides, the activity can be further increased, which enriched the number of active sites in these carbons.

Despite of functionalization, another strategy of surface modifications is combining macromolecules with carbons, such as organic chains and polymers. Inspired by such concepts, our group innovatively proposed a polymer-carbon modification route, which improved 2e-ORR selectivity by establishing polydopamine (PDA)-defective carbon (CB-PDA-A) electrocatalytic system [53]. The FE of the CB-PDA-A reached nearly 100% at 0.5 V_{RHE}, harvesting an industrial-level H_2O_2 yield of 1.8 mol g_{cat}^{-1} h^{-1}. Experimental results revealed that the improved ORR activity and selectivity were caused by the tuned electronic structure, due to the non-covalent dipole-dipole interaction between PDA polymers and defective carbon sites. Such electronic polarization from PDA restructured the electronic configuration of local carbon active sites, thus maintaining O–O bonds of OOH intermediate and leading to reinforced 2e-ORR selectivity as revealed by well-designed anaerobic tests (Figure 5d). Besides, the desorption efficiency of the *OOH intermediate at the active site could also be another factor to affect 2e-selectivity. Some conventional cationic surfactants, such as cetyltrimethylammonium bromide (CTAB), were utilized to decorate metal-free carbon surfaces [54]. More than 95% H_2O_2 selectivity was obtained on the

catalyst within a wide voltage range of 0.7–0.1 V_{RHE}. Due to the local Coulomb effect of the CTAB layer, the *OOH intermediates adsorbed on the catalyst surface were forced to be desorbed before their further reduction (4e-ORR), thus outcoming high H_2O_2 selectivity (Figure 5e).

In addition to the above thermodynamic approaches, the ORR procedures in the vicinity of the carbon active sites could be tailored by regulating the microenvironments of the carbon interfaces. For instance, Zhang et al. controlled the interface hydrophilicity of a carbon fiber cloth through loading polytetrafluoroethylene (PTFE)-protected carbon black [55]. Compared with the pristine carbon cloth, the formation of superhydrophobic air diffusion layers resulted in an accelerated mass exchanging with an increment of 5.7 times quicker O_2 diffusion from ambient air to the reaction interfaces. However, excessive PTFE would lead to a reduction of active sites and hindered ion transfer, and the enrichment of protons in the acidic electrolyte in turn could cause further reduction to H_2O. To this end, Wang et al. reported a cation-modulated catalyst/electrolyte interface to realize highly selective and effective electrochemical reduction of O_2 to H_2O_2 in acids [56]. Molecular dynamics simulations echoed with experimental results demonstrated that solvated alkali metal cations (such as Na^+) could be preferentially attracted on the electrical double layer interfaces between carbon catalysts/electrolyte and extruded localized protons during the reactions. Such cation shielding squeezed away protons and inhibited the further reduction of the generated H_2O_2 (Figure 5f).

Collectively, it is worth noting that the design and regulation on interfaces between carbons and electrolytes are still rarely seen in recent publications, which in fact poses significant influences on the overall energy efficiency of the whole electrocatalytic process. It could also be governed by innovative designs on device and electrolyte types, which is however beyond the scope of this review [105–107].
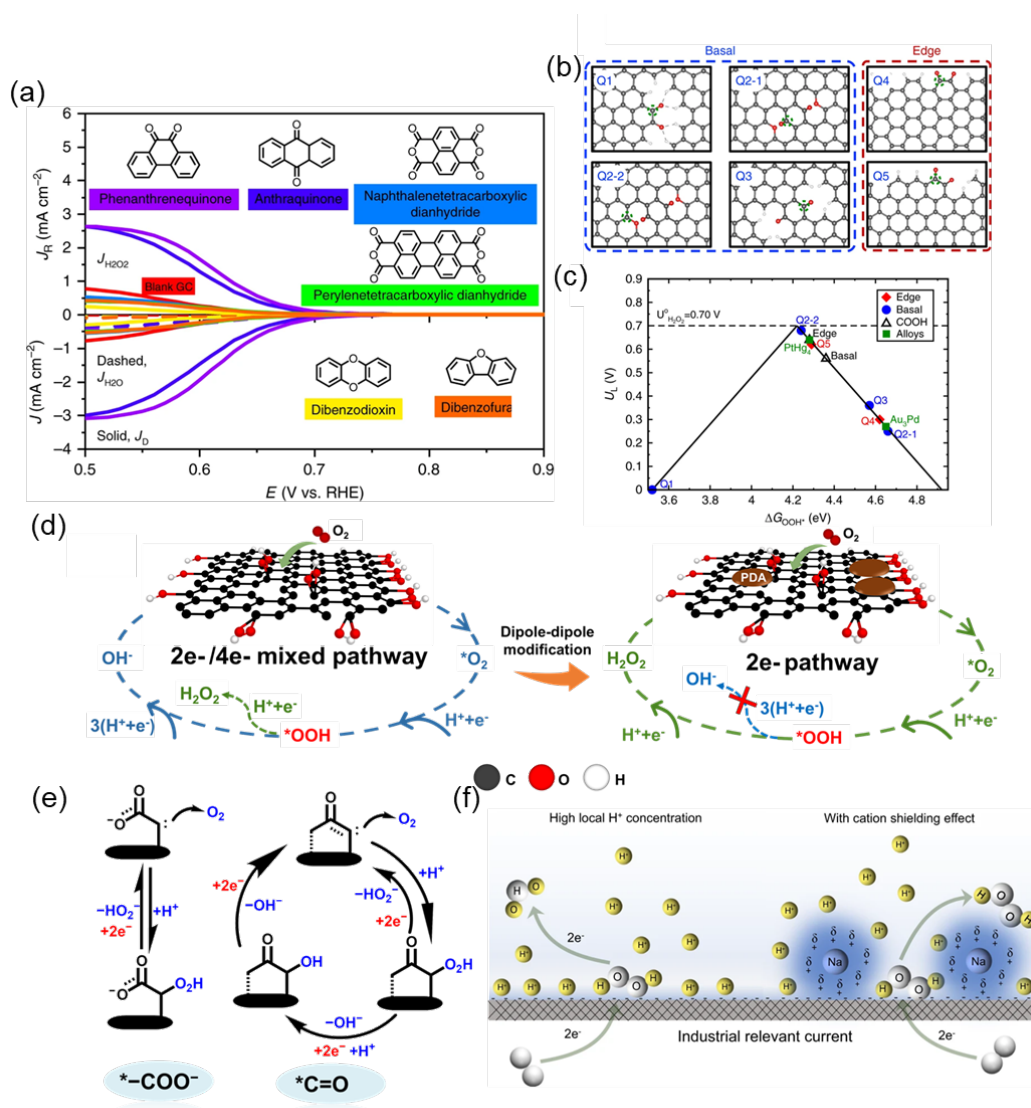

Figure 5. (**a**) Comparison of RRDE currents of the quinone species and blank glassy carbon (GC). (**b**) DFT results of the oxygen functional groups. (**c**) Theoretical 2e-ORR activity volcano plot [51]. (**d**) Schematic mechanism of

the ORR selectivity with dipole-dipole interaction [53]. (**e**) A simplified reaction pathways at carbonyl and carboxyl sites. Originally re-drawn and concept from Ref. [50]. (**f**) Schematic diagram of 2e-ORR in acid with/without Na^+ adsorption over carbon catalysts [56].

5. Conclusions and Perspective

The two-electron oxygen electrochemical reduction is becoming more promising in recent years, due to its potential high faradaic efficiency and considerable productivity. Still, 2e-ORR on carbon-based materials is demanding substantial progress to further enhance the catalytic activity, selectivity, and stability. Thus, in-depth understandings of the active sites for 2e-ORR are of great importance. This review has summarized the recent progress of carbon-based active sites in 2e-ORR, including the doping sites, defective sites, and modified surfaces. At the same time, the electron transfer mechanism of the catalytic active site and the intermediate *OOH has a great influence on 2e-ORR. Based on this, the researchers optimized existing materials through interface engineering to design specific functional groups on the carbon surface to accelerate the desorption of H_2O_2, thereby further improving the selectivity of H_2O_2.Based on such findings, innovations on the design and development of novel carbon catalysts are extremely applaudable. The brief report reviews the development of catalysts and their underlying mechanism of active sites for electrocatalytic H_2O_2 production. Despite the pioneer work and achievements that have been reviewed, there are still many opportunities for the electrochemical conversion of O_2-to-H_2O_2. Specific challenges and potential strategies are briefly discussed as follows:

1) Electronic engineering on the ORR-active sites of carbon-based catalysts for efficient and stable 2e-ORR. To suppress the thermodynamically preferential 4-electron pathway, the combination of catalytic carbon and electro-withdrawing species, such as chalcogen and their functional groups, would be a feasible solution. Meanwhile, the coordination manipulation is another practical method to promote the 2e-ORR performance of carbons. Manipulating the defects and porous topology together with heteroatom doping would also help with the design and optimization of the carbon catalysts. It not only dynamically facilitates the 2e-route but also boosts the mass diffusion for application purposes. Meanwhile, due to the vulnerability of carbon active sites in acid media, the carbon-based catalysts with superior 2e-ORR in acid is still rare, while metal-free carbons have intrinsic advantages in harsh acidic environment over metal or metal compounds. Also, H_2O_2 is rather stable in acids than in alkaline. Therefore, it is of great opportunities and challenges to fabricate acidic carbon catalysts for acidic H_2O_2 production.

2) Mechanism study of the carbon-based catalysts for H_2O_2 electro-synthesis *via in-situ* and *Operando* techniques. Most of the efforts are still concentrated on the improvement of catalytic performance, whereas the underlying mechanism of the 2e-ORR is rarely investigated in-depth. One of the possible reasons is that 2e-ORR shares similar mechanism to 4e-ORR, which has been studied extensively in the fuel-cell-related investigations [108,109]. Thus, in most cases, the same methodology has been employed in theoretical simulations and calculations in both 2e-ORR and 4e-ORR. However, the 2e-ORR may employ fewer intermediates and peroxides products could feature different decomposition routes, either of which leads to a distinct and complex mechanism compared with 4e-pathway. Therefore, advanced characterizations, especially *in-situ* and *Operando* techniques with atomic resolutions, are strongly encouraged to be applied in unveiling the 2e-ORR mechanism. It would be useful and practical guidelines for future design of carbon catalysts.

3) Device innovations for chemical and environmental purposes. Aside from the catalytic materials, optimizations of GDE or membrane electrode assembly (MEA) for practical applications is greatly significant. Nevertheless, limited research is conducted towards GDEs or MEAs on carbon catalysts for 2e-ORR. One of the main reasons is the device performance of the assembled GDEs and MEAs are considerably inferior to their RRDE activity, predominately due to the dramatic differences in electrolytes and mass transfer properties. In this case, the catalytic behaviors of the carbon active sites would be kinetically and thermodynamically changes. Therefore, based on unveiling the correlation between the media environments, mass transfer simulations and performance, the novel fabrications of device could be further advanced to meet practical and economic ambitions.

Conflicts of Interest: The authors declare no conflict of interest.

References

1. Zhang, Q.; Chen, Y.; Pan, J.; Daiyan, R.; Lovell, E.C.; Yun, J.; Amal, R.; Lu, X. Electrosynthesis of Hydrogen Peroxide through Selective Oxygen Reduction: A Carbon Innovation from Active Site Engineering to Device Design. *Small* **2023**, *19*(40), 2302338.

2. Hydrogen Peroxide Market Size & Share Report, 2021–2028. Available online: https://www.grandviewresearch.com/industry-analysis/hydrogen-peroxide-market (accessed on 15 January 2024).

3. Xia, C.; Kim, J.Y.; Wang, H. Recommended Practice to Report Selectivity in Electrochemical Synthesis of H_2O_2. *Nat. Catal.* **2020**, *3*(8), 605.

4. Yang, S.; Verdaguer-Casadevall, A.; Arnarson, L.; Silvioli, L.; Čolić, V.; Frydendal, R.; Rossmeisl, J.; Chorkendorff, I.; Stephens, I.E.L. Toward the Decentralized Electrochemical Production of H_2O_2: A Focus on the Catalysis. *ACS Catal.* **2018**, *8*(5), 4064.

5. Wei, Z.; Zhao, S.; Li, W.; Zhao, X.; Chen, C.; Phillips, D.L.; Zhu, Y.; Choi, W. Artificial Photosynthesis of H_2O_2 through Reversible Photoredox Transformation between Catechol and o-Benzoquinone on Polydopamine-coated CdS. *ACS Catal.* **2022**, *12*(18), 11436.

6. Li, W.; Wei, Z.; Sheng, Y.; Xu, J.; Ren, Y.; Jing, J.; Yang, J.; Li, J.; Zhu, Y. Dual Cocatalysts Synergistically Promote Perylene Diimide Polymer Charge Transfer for Enhanced Photocatalytic Water Oxidation. *ACS Energy Lett.* **2023**, *8*(6), 2652.

7. Wei, Z.; Liu, M.; Zhang, Z.; Yao, W.; Tan, H.; Zhu, Y. Efficient Visible-light-driven Selective Oxygen Reduction to Hydrogen Peroxide by Oxygen-enriched Graphitic Carbon Nitride Polymers. *Energy Environ. Sci.* **2018**, *11*(9), 2581.

8. Zhang, L.; Liang, J.; Yue, L.; Xu, Z.; Dong, K.; Liu, Q.; Luo, Y.; Li, T.; Cheng, X.; Cui, G.; et al. N-doped Carbon Nanotubes Supported $CoSe_2$ Nanoparticles: A Highly Efficient and Stable Catalyst for H_2O_2 Electrosynthesis in Acidic Media. *Nano Re*s. **2022**, *15*(1), 304.

9. Tian, Y.; Deng, D.; Xu, L.; Li, M.; Chen, H.; Wu, Z.; Zhang, S. Strategies for Sustainable Production of Hydrogen Peroxide via Oxygen Reduction Reaction: From Catalyst Design to Device Setup. *Nanomicro Lett* **2023**, *15*(1), 122.

10. Wang, D.; Li, S.; Zhang, X.; Feng, B.; Pei, Y.; Zhu, Y.; Xu, W.; Li, Z.-H.; Qiao, M.; Zong, B. Pyrolyzed Polydopamine-modified Carbon Black for Selective and Durable Electrocatalytic Oxygen Reduction to Hydrogen Peroxide in Acidic Medium. *Appl. Catal. B* **2022**, *305*, 121036.

11. Sa, Y.J.; Kim, J.H.; Joo, S.H. Active Edge-Site-Rich Carbon Nanocatalysts with Enhanced Electron Transfer for Efficient Electrochemical Hydrogen Peroxide Production. *Angew. Chem. Int. Ed.* **2019**, *58*(4), 1100.

12. Zhang, D.; Wang, Z.; Liu, F.; Yi, P.; Peng, L.; Chen, Y.; Wei, L.; Li, H. Unraveling the pH-Dependent Oxygen Reduction Performance on Single-Atom Catalysts: From Single- to Dual-Sabatier Optima. *J. Am. Chem. Soc.* **2024**, *146*, 3210–3219. https://doi.org/10.1021/jacs.3c11246 10.1021/jacs.3c11246.

13. Zhang, T.; Wu, J.; Wang, Z.; Wei, Z.; Liu, J.; Gong, X. Transfer of Molecular Oxygen and Electrons Improved by the Regulation of C-N/C=O for Highly Efficient 2e-ORR. *Chem. Eng. J.* **2022**, *433*, 133591.

14. Wang, Z.; Li, Q.-K.; Zhang, C.; Cheng, Z.; Chen, W.; McHugh, E.A.; Carter, R.A.; Yakobson, B.I.; Tour, J.M. Hydrogen Peroxide Generation with 100% Faradaic Efficiency on Metal-Free Carbon Black. *ACS Catal.* **2021**, *11*(4), 2454.

15. Chang, Q.; Zhang, P.; Mostaghimi, A.H.B.; Zhao, X.; Denny, S.R.; Lee, J.H.; Gao, H.; Zhang, Y.; Xin, H.L.; Siahrostami, S.; et al. Promoting H_2O_2 Production via 2-electron Oxygen Reduction by Coordinating Partially Oxidized Pd with Defect Carbon. *Nat. Commun.* **2020**, *11*(1), 2178.

16. Du, J.; Jiang, S.; Zhang, R.; Wang, P.; Ma, C.; Zhao, R.; Cui, C.; Zhang, Y.; Kang, Y. Generation of Pd–O for Promoting Electrochemical H_2O_2 Production. *ACS Catal.* **2023**, *13*(10), 6887.

17. Yang, H.; Wang, B.; Li, H.; Ni, B.; Wang, K.; Zhang, Q.; Wang, X. Trimetallic Sulfide Mesoporous Nanospheres as Superior Electrocatalysts for Rechargeable Zn–Air Batteries. *Adv. Energy Mater.* **2018**, *8*(34), 1801839.

18. Xia, F.; Li, B.; Liu, Y.; Liu, Y.; Gao, S.; Lu, K.; Kaelin, J.; Wang, R.; Marks, T.J.; Cheng, Y. Carbon Free and Noble Metal Free $Ni_2Mo_6S_8$ Electrocatalyst for Selective Electrosynthesis of H_2O_2. *Adv. Funct. Mater.* **2021**, *31*(47), 2104716.

19. Zhang, L.; Liang, J.; Yue, L.; Dong, K.; Xu, Z.; Li, T.; Liu, Q.; Luo, Y.; Liu, Y.; Gao, S.; et al. CoTe Nanoparticle-Embedded N-doped Hollow Carbon Polyhedron: An Efficient Catalyst for H_2O_2 Electrosynthesis in Acidic Media. *J. Mater. Chem. A* **2021**, *9*(38), 21703.

20. Song, M.; Liu, W.; Zhang, J.; Zhang, C.; Huang, X.; Wang, D. Single-Atom Catalysts for H_2O_2 Electrosynthesis via Two-Electron Oxygen Reduction Reaction. *Adv. Funct. Mater.* **2023**, *33*(15), 2212087.

21. Xiao, C.; Cheng, L.; Zhu, Y.; Wang, G.; Chen, L.; Wang, Y.; Chen, R.; Li, Y.; Li, C. Super-Coordinated Nickel $N_4Ni_1O_2$ Site Single-Atom Catalyst for Selective H_2O_2 Electrosynthesis at High Current Densities. *Angew. Chem. Int. Ed.* **2022**,

61(38), e202206544.

22. Wang, N.; Ma, S.; Zuo, P.; Duan, J.; Hou, B. Recent Progress of Electrochemical Production of Hydrogen Peroxide by Two-Electron Oxygen Reduction Reaction. *Adv. Sci.* **2021**, *8*(15), 2100076.

23. Zhao, H.; Yuan, Z.-Y. Design Strategies of Non-Noble Metal-Based Electrocatalysts for Two-Electron Oxygen Reduction to Hydrogen Peroxide. *ChemSusChem* **2021**, *14*(7), 1616.

24. Bu, Y.; Wang, Y.; Han, G.-F.; Zhao, Y.; Ge, X.; Li, F.; Zhang, Z.; Zhong, Q.; Baek, J.-B. Carbon-Based Electrocatalysts for Efficient Hydrogen Peroxide Production. *Adv. Mater.* **2021**, *33*(49), 2103266.

25. Hu, C.; Paul, R.; Dai, Q.; Dai, L. Carbon-based Metal-free Electrocatalysts: From Oxygen Reduction to Multifunctional Electrocatalysis. *Chem. Soc. Rev.* **2021**, *50*(21), 11785.

26. Long, Y.; Lin, J.; Ye, F.; Liu, W.; Wang, D.; Cheng, Q.; Paul, R.; Cheng, D.; Mao, B.; Yan, R.; et al. Tailoring the Atomic-Local Environment of Carbon Nanotube Tips for Selective H$_2$O$_2$ Electrosynthesis at High Current Densities. *Adv. Mater.* **2023**, *35*(46), 2303905.

27. He, H.; Liu, S.; Liu, Y.; Zhou, L.; Wen, H.; Shen, R.; Zhang, H.; Guo, X.; Jiang, J.; Li, B. Review and Perspectives on Carbon-based Electrocatalysts for the Production of H$_2$O$_2$ via Two-electron Oxygen Reduction. *Green Chem.* **2023**, *25*(23), 9501.

28. Wei, L.; Dong, Z.; Chen, R.; Wu, Q.; Li, J. Review of Carbon-based Nanocomposites as Electrocatalyst for H$_2$O$_2$ Production from Oxygen. *Ionics* **2022**, *28*(9), 4045.

29. Peng, W.; Liu, J.; Liu, X.; Wang, L.; Yin, L.; Tan, H.; Hou, F.; Liang, J. Facilitating Two-electron Oxygen Reduction with Pyrrolic Nitrogen Sites for Electrochemical Hydrogen Peroxide Production. *Nat. Commun.* **2023**, *14*(1), 4430.

30. Yang, Y.; He, F.; Shen, Y.; Chen, X.; Mei, H.; Liu, S.; Zhang, Y. A Biomass Derived N/C-catalyst for the Electrochemical Production of Hydrogen Peroxide. *Chem. Commun.* **2017**, *53*(72), 9994.

31. Zhang, J.; Zhang, G.; Jin, S.; Zhou, Y.; Ji, Q.; Lan, H.; Liu, H.; Qu, J. Graphitic N in Nitrogen-Doped Carbon Promotes Hydrogen Peroxide Synthesis from Electrocatalytic Oxygen Reduction. *Carbon* **2020**, *163*, 154.

32. Chen, G.; Liu, J.; Qingqing, l.; Guan, P.; Yu, X.; Xing, L.; Zhang, J.; Che, R. A Direct H$_2$O$_2$ Production Based on Hollow Porous Carbon Sphere-sulfur Nanocrystal Composites by Confinement Effect as Oxygen Reduction Electrocatalysts. *Nano Res.* **2019**, *12*, 2614–2622.

33. Jia, N.; Yang, T.; Shi, S.; Chen, X.; An, Z.; Chen, Y.; Yin, S.; Chen, P. N,F-codoped Carbon Nanocages: An Efficient Electrocatalyst for Hydrogen Peroxide Electroproduction in Alkaline and Acidic Solutions. *ACS Sustain. Chem. Eng.* **2020**, *8*(7), 2883.

34. Li, L.; Tang, C.; Zheng, Y.; Xia, B.; Zhou, X.; Xu, H.; Qiao, S.-Z. Tailoring Selectivity of Electrochemical Hydrogen Peroxide Generation by Tunable Pyrrolic-Nitrogen-Carbon. *Adv. Energy Mater.* **2020**, *10*(21), 2000789.

35. Wan, J.; Zhang, G.; Hongrun, J.; Wu, J.; Zhang, N.; Yao, B.; Liu, K.; Liu, M.; Liu, T.; Huang, L. Microwave-assisted Synthesis of Well-defined Nitrogen Doping Configuration with High Centrality in Carbon to Identify the Active Sites for Electrochemical Hydrogen Peroxide Production. *Carbon* **2022**, *191*, 340–349.

36. Ri, K.; Pak, S.; Sun, D.; Zhong, Q.; Yang, S.; Sin, S.; Wu, L.; Sun, Y.; Cao, H.; Han, C.; et al. Boron-doped rGO Electrocatalyst for High Effective Generation of Hydrogen Peroxide: Mechanism and Effect of Oxygen-enriched Air. *Appl. Catal. B* **2024**, *343*, 123471.

37. Xiang, F.; Zhao, X.; Yang, J.; Li, N.; Gong, W.; Liu, Y.; Burguete-Lopez, A.; Li, Y.; Niu, X.; Fratalocchi, A. Enhanced Selectivity in the Electroproduction of H$_2$O$_2$ via F/S Dual-Doping in Metal-Free Nanofibers. *Adv. Mater.* **2023**, *35*(7), 2208533.

38. Xia, Y.; Zhao, X.; Xia, C.; Wu, Z.-Y.; Zhu, P.; Kim, J.Y.; Bai, X.; Gao, G.; Hu, Y.; Zhong, J.; et al. Highly Active and Selective Oxygen Reduction to H$_2$O$_2$ on Boron-doped Carbon for High Production Rates. *Nat. Commun.* **2021**, *12*(1), 4225.

39. Chen, S.; Chen, Z.; Siahrostami, S.; Kim, T.R.; Nordlund, D.; Sokaras, D.; Nowak, S.; To, J.W.F.; Higgins, D.; Sinclair, R.; et al. Defective Carbon-Based Materials for the Electrochemical Synthesis of Hydrogen Peroxide. *ACS Sustain. Chem. Eng.* **2018**, *6*(1), 311.

40. Lee, K.; Lim, J.; Lee, M.J.; Ryu, K.; Lee, H.; Kim, J.Y.; Ju, H.; Cho, H.-S.; Kim, B.-H.; Hatzell, M.C.; et al. Structure-controlled Graphene Electrocatalysts for High-performance H$_2$O$_2$ Production. *Energy Environ. Sci.* **2022**, *15*(7), 2858.

41. Zhang, C.; Shen, W.; Guo, K.; Xiong, M.; Zhang, J.; Lu, X. A Pentagonal Defect-Rich Metal-Free Carbon Electrocatalyst for Boosting Acidic O$_2$ Reduction to H$_2$O$_2$ Production. *J. Am. Chem. Soc.* **2023**, *145*(21), 11589.

42. Shen, W.; Zhang, C.; Wang, X.; Huang, Y.; Du, Z.; Alomar, M.; Wang, J.; Lv, J.; Zhang, J.; Lu, X. Sulfur-Doped Defective Nanocarbons Derived from Fullerenes as Electrocatalysts for Efficient and Selective H$_2$O$_2$ Electroproduction. *ACS Mater. Lett.* **2024**, *6*(1), 17.

43. Wu, Q.; Zou, H.; Mao, X.; He, J.; Shi, Y.; Chen, S.; Yan, X.; Wu, L.; Lang, C.; Zhang, B.; et al. Unveiling the Dynamic Active Site of Defective Carbon-based Electrocatalysts for Hydrogen Peroxide Production. *Nat. Commun.* **2023**, *14*(1), 6275.

44. Wang, W.; Zheng, Y.; Hu, Y.; Liu, Y.; Chen, S. Intrinsic Carbon Defects for the Electrosynthesis of H₂O₂. The *J. Phys. Chem. Lett.* **2022**, *13*(38), 8914.

45. Dong, K.; Liang, J.; Wang, Y.; Xu, Z.; Liu, Q.; Luo, Y.; Li, T.; Li, L.; Shi, X.; Asiri, A.M.; et al. Honeycomb Carbon Nanofibers: A Superhydrophilic O₂-Entrapping Electrocatalyst Enables Ultrahigh Mass Activity for the Two-Electron Oxygen Reduction Reaction. *Angew. Chem. Int. Ed.* **2021**, *60*(19), 10583.

46. Fan, M.; Wang, Z.; Sun, K.; Wang, A.; Zhao, Y.; Yuan, Q.; Wang, R.; Raj, J.; Wu, J.; Jiang, J.; et al. N-B-OH Site-Activated Graphene Quantum Dots for Boosting Electrochemical Hydrogen Peroxide Production. *Adv. Mater.* **2023**, *35*(17), 2209086.

47. Jing, L.; Tian, Q.; Li, X.; Sun, J.; Wang, W.; Yang, H.; Chai, X.; Hu, Q.; He, C. Dual-Engineering of Porous Structure and Carbon Edge Enables Highly Selective H₂O₂ Electrosynthesis. *Adv. Funct. Mater.* **2023**, *33*(47), 2305795.

48. Zhang, D.; Tsounis, C.; Ma, Z.; Djaidiguna, D.; Bedford, N.M.; Thomsen, L.; Lu, X.; Chu, D.; Amal, R.; Han, Z. Highly Selective Metal-Free Electrochemical Production of Hydrogen Peroxide on Functionalized Vertical Graphene Edges. *Small* **2022**, *18*(1), 2105082.

49. Kim, H.W.; Ross, M.B.; Kornienko, N.; Zhang, L.; Guo, J.; Yang, P.; McCloskey, B.D. Efficient Hydrogen Peroxide Generation Using Reduced Graphene Oxide-based Oxygen Reduction Electrocatalysts. *Nat. Catal.* **2018**, *1*(4), 282.

50. Lu, Z.; Chen, G.; Siahrostami, S.; Chen, Z.; Liu, K.; Xie, J.; Liao, L.; Wu, T.; Lin, D.; Liu, Y.; et al. High-efficiency Oxygen Reduction to Hydrogen Peroxide Catalysed by Oxidized Carbon Materials. *Nat. Catal.* **2018**, *1*(2), 156.

51. Han, G.-F.; Li, F.; Zou, W.; Karamad, M.; Jeon, J.-P.; Kim, S.-W.; Kim, S.-J.; Bu, Y.; Fu, Z.; Lu, Y.; et al. Building and Identifying Highly Active Oxygenated Groups in Carbon Materials for Oxygen Reduction to H₂O₂. *Nat. Commun.* **2020**, *11*(1), 2209.

52. Zhang, H.; Li, Y.; Zhao, Y.; Li, G.; Zhang, F. Carbon Black Oxidized by Air Calcination for Enhanced H₂O₂ Generation and Effective Organics Degradation. *ACS Appl. Mater. Interfaces* **2019**, *11*(31), 27846.

53. Su, J.; Jiang, L.; Xiao, B.; Liu, Z.; Wang, H.; Zhu, Y.; Wang, J.; Zhu, X. Dipole–Dipole Tuned Electronic Reconfiguration of Defective Carbon Sites for Efficient Oxygen Reduction into H₂O₂. *Small*. https://doi.org/10.1002/smll.202310317, 2310317.

54. Wu, K.-H.; Wang, D.; Lu, X.; Zhang, X.; Xie, Z.; Liu, Y.; Su, B.-J.; Chen, J.-M.; Su, D.-S.; Qi, W.; et al. Highly Selective Hydrogen Peroxide Electrosynthesis on Carbon: In Situ Interface Engineering with Surfactants. *Chem* **2020**, *6*(6), 1443.

55. Zhang, Q.; Zhou, M.; Ren, G.; Li, Y.; Li, Y.; Du, X. Highly Efficient Electrosynthesis of Hydrogen Peroxide on a Superhydrophobic Three-phase Interface by Natural Air Diffusion. *Nat. Commun.* **2020**, *11*(1), 1731.

56. Zhang, X.; Zhao, X.; Zhu, P.; Adler, Z.; Wu, Z.-Y.; Liu, Y.; Wang, H. Electrochemical Oxygen Reduction to Hydrogen Peroxide at Practical Rates in Strong Acidic Media. *Nat. Commun.* **2022**, *13*(1), 2880.

57. Cui, L.; Chen, B.; Zhang, L.; He, C.; Shu, C.; Kang, H.; Qiu, J.; Jing, W.; Ostrikov, K.; Zhang, Z. An Anti-electrowetting Carbon Film Electrode with Self-sustained Aeration for Industrial H₂O₂ Electrosynthesis. *Energy Environ. Sci.* **2024**, *17*, 655–667. https://doi.org/10.1039/D3EE03223J 10.1039/D3EE03223J.

58. Zhu, X.; Hu, C.; Amal, R.; Dai, L.; Lu, X. Heteroatom-doped Carbon Catalysts for Zinc–Air Batteries: Progress, Mechanism, and Opportunities. *Energy Environ. Sci.* **2020**, *13*(12), 4536.

59. Wohlgemuth, S.-A.; White, R.J.; Willinger, M.-G.; Titirici, M.-M.; Antonietti, M. A One-pot Hydrothermal Synthesis of Sulfur and Nitrogen Doped Carbon Aerogels with Enhanced Electrocatalytic Activity in the Oxygen Reduction Reaction. *Green Chem.* **2012**, *14*(5), 1515.

60. Sheng, X.; Daems, N.; Geboes, B.; Kurttepeli, M.; Bals, S.; Breugelmans, T.; Hubin, A.; Vankelecom, I.F.J.; Pescarmona, P.P. N-doped Ordered Mesoporous Carbons Prepared by a Two-step Nanocasting Strategy as Highly Active and Selective Electrocatalysts for the Reduction of O₂ to H₂O₂. *Appl. Catal. B* **2015**, *176–177*, 212–224.

61. Singh, S.K.; Takeyasu, K.; Nakamura, J. Active Sites and Mechanism of Oxygen Reduction Reaction Electrocatalysis on Nitrogen-Doped Carbon Materials. *Adv. Mater.* **2019**, *31*(13), 1804297.

62. Fellinger, T.-P.; Hasché, F.; Strasser, P.; Antonietti, M. Mesoporous Nitrogen-Doped Carbon for the Electrocatalytic Synthesis of Hydrogen Peroxide. *J. Am. Chem. Soc.* **2012**, *134*(9), 4072.

63. Miao, H.; Li, S.H.; Wang, Z.H.; Sun, S.S.; Kuang, M.; Liu, Z.P.; Yuan, J.L. Enhancing the Pyridinic N Content of Nitrogen-doped Graphene and Improving its Catalytic Activity for Oxygen Reduction Reaction. *Int. J. Hydrogen Energy* **2017**, *42*(47), 28298.

64. Wu, J.J.; Ma, L.L.; Yadav, R.M.; Yang, Y.C.; Zhang, X.; Vajtai, R.; Lou, J.; Ajayan, P.M. Nitrogen-Doped Graphene with Pyridinic Dominance as a Highly Active and Stable Electrocatalyst for Oxygen Reduction. *ACS Appl. Mater. Interfaces* **2015**, *7*(27), 14763.

65. Kong, F.; Cui, X.; Huang, Y.; Yao, H.; Chen, Y.; Tian, H.; Meng, G.; Chen, C.; Chang, Z.; Shi, J. N-Doped Carbon Electrocatalyst: Marked ORR Activity in Acidic Media without the Contribution from Metal Sites? *Angew. Chem. Int. Ed.* **2022**, *61*(15), e202116290.

66. Zhang, J.; Sun, Y.; Zhu, J.; Kou, Z.; Hu, P.; Liu, L.; Li, S.; Mu, S.; Huang, Y. Defect and Pyridinic Nitrogen Engineering

of Carbon-based Metal-free Nanomaterial Toward Oxygen Reduction. *Nano Energy* **2018**, *52*, 307.

67. Tuci, G.; Zafferoni, C.; D'Ambrosio, P.; Caporali, S.; Ceppatelli, M.; Rossin, A.; Tsoufis, T.; Innocenti, M.; Giambastiani, G. Tailoring Carbon Nanotube N-Dopants while Designing Metal-Free Electrocatalysts for the Oxygen Reduction Reaction in Alkaline Medium. *ACS Catal.* **2013**, *3*(9), 2108.

68. Wan, K.; Long, G.-F.; Liu, M.-Y.; Du, L.; Liang, Z.-X.; Tsiakaras, P. Nitrogen-doped Ordered Mesoporous Carbon: Synthesis and Active sites for Electrocatalysis of Oxygen Reduction Reaction. *Appl. Catal. B* **2015**, *165*, 566.

69. Iglesias, D.; Giuliani, A.; Melchionna, M.; Marchesan, S.; Criado, A.; Nasi, L.; Bevilacqua, M.; Tavagnacco, C.; Vizza, F.; Prato, M.; et al. N-Doped Graphitized Carbon Nanohorns as a Forefront Electrocatalyst in Highly Selective O_2 Reduction to H_2O_2. *Chem* **2018**, *4*(1), 106.

70. Sun, Y.; Li, S.; Jovanov, Z.P.; Bernsmeier, D.; Wang, H.; Paul, B.; Wang, X.; Kühl, S.; Strasser, P. Structure, Activity, and Faradaic Efficiency of Nitrogen-Doped Porous Carbon Catalysts for Direct Electrochemical Hydrogen Peroxide Production. *ChemSusChem* **2018**, *11*(19), 3388.

71. Rao, C.V.; Cabrera, C.R.; Ishikawa, Y. In Search of the Active Site in Nitrogen-Doped Carbon Nanotube Electrodes for the Oxygen Reduction Reaction. *J. Phys. Chem. Lett.* **2010**, *1*, 2622.

72. Yu, S.-S.; Zheng, W.-T. Effect of N/B Doping on the Electronic and Field Emission Properties for Carbon Nanotubes, Carbon Nanocones, and Graphene Nanoribbons. *Nanoscale* **2010**, *2*(7), 1069.

73. Meyer, J.C.; Kurasch, S.; Park, H.J.; Skakalova, V.; Künzel, D.; Groß, A.; Chuvilin, A.; Algara-Siller, G.; Roth, S.; Iwasaki, T.; et al. Experimental Analysis of Charge Redistribution due to Chemical Bonding by High-Resolution Transmission Electron Microscopy. *Nat. Mater.* **2011**, *10*(3), 209.

74. Kondo, T.; Casolo, S.; Suzuki, T.; Shikano, T.; Sakurai, M.; Harada, Y.; Saito, M.; Oshima, M.; Trioni, M.I.; Tantardini, G. F.; et al. Atomic-scale Characterization of Nitrogen-doped Graphite: Effects of Dopant Nitrogen on the Local Electronic Structure of the Surrounding Carbon Atoms. *Phys. Rev. B* **2012**, *86*(3), 035436.

75. Roldán, L.; Truong-Phuoc, L.; Ansón-Casaos, A.; Pham-Huu, C.; García-Bordejé, E. Mesoporous Carbon Doped with N,S Heteroatoms Prepared by One-pot Auto-assembly of Molecular Precursor for Electrocatalytic Hydrogen Peroxide Synthesis. *Catal. Today* **2018**, *301*, 2–10.

76. He, W.; Wang, Y.; Jiang, C.; Lu, L. Structural Effects of a Carbon Matrix in Non-precious Metal O_2-reduction Electrocatalysts. *Chem. Soc. Rev.* **2016**, *45*(9), 2396.

77. Zhao, K.; Su, Y.; Quan, X.; Liu, Y.; Chen, S.; Yu, H. Enhanced H_2O_2 Production by Selective Electrochemical Reduction of O_2 on Fluorine-doped Hierarchically Porous Carbon. *J. Catal.* **2018**, *357*, 118.

78. Wang, W.; Lu, X.; Su, P.; Li, Y.; Cai, J.; Zhang, Q.; Zhou, M.; Arotiba, O. Enhancement of Hydrogen Peroxide Production by Electrochemical Reduction of Oxygen on Carbon Nanotubes Modified with Fluorine. *Chemosphere* **2020**, *259*, 127423.

79. Jang, A.R.; Lee, Y.-W.; Lee, S.-S.; Hong, J.; Beak, S.-H.; Pak, S.; Lee, J.; Shin, H.S.; Ahn, D.; Hong, W.-K.; et al. Electrochemical and Electrocatalytic Reaction Characteristics of Boron-incorporated Graphene via a Simple Spin-on Dopant Process. *J. Mater. Chem. A* **2018**, *6*(17), 7351.

80. Yu, X.; Han, P.; Wei, Z.; Huang, L.; Gu, Z.; Peng, S.; Ma, J.; Zheng, G. Boron-Doped Graphene for Electrocatalytic N_2 Reduction. *Joule* **2018**, *2*(8), 1610.

81. Vineesh, T.V.; Kumar, M.P.; Takahashi, C.; Kalita, G.; Alwarappan, S.; Pattanayak, D.K.; Narayanan, T.N. Bifunctional Electrocatalytic Activity of Boron-Doped Graphene Derived from Boron Carbide. *Adv. Energy Mater.* **2015**, *5*(17), 1500658.

82. Liu, L.; Yan, C.; Luo, X.; Li, C.; Zhang, D.; Peng, H.; Wang, H.; Zheng, B.; Guo, Y. Phosphorus Doped Hierarchical Porous Carbon: An Efficient Oxygen Reduction Electrocatalyst for On-site H_2O_2 Production. *Inorg. Chem. Front.* **2023**, *10*(12), 3632.

83. Gu, Y.-y.; Fu, H.; Huang, Z.; Lin, R.; Wu, Z.; Li, M.; Cui, Y.; Fu, R.; Wang, S. O/F Co-doped CNTs Promoted Graphite Felt Gas Diffusion Cathode for Highly Efficient and Durable H_2O_2 Evolution without Aeration. *J. Clean. Prod.* **2022**, *341*, 130799.

84. Ji, L.; Rao, M.; Zheng, H.; Zhang, L.; Li, Y.; Duan, W.; Guo, J.; Cairns, E.J.; Zhang, Y. Graphene Oxide as a Sulfur Immobilizer in High Performance Lithium/Sulfur Cells. *J. Am. Chem. Soc.* **2011**, *133*(46), 18522.

85. Paraknowitsch, J.P.; Thomas, A. Doping Carbons Beyond Nitrogen: An Overview of Advanced Heteroatom Doped Carbons with Boron, Sulphur and Phosphorus for Energy Applications. *Energy Environ. Sci.* **2013**, *6*(10), 2839.

86. Zhu, C.; Li, H.; Fu, S.; Du, D.; Lin, Y. Highly Efficient Nonprecious Metal Catalysts Towards Oxygen Reduction Reaction Based on Three-dimensional Porous Carbon Nanostructures. *Chem. Soc. Rev.* **2016**, *45*(3), 517.

87. Feng, X.; Bai, Y.; Liu, M.; Li, Y.; Yang, H.; Wang, X.; Wu, C. Untangling the Respective Effects of Heteroatom-doped Carbon Materials in Batteries, Supercapacitors and the ORR to Design High Performance Materials. *Energy Environ. Sci.* **2021**, *14*(4), 2036.

88. Hu, C.; Dai, L. Doping of Carbon Materials for Metal-Free Electrocatalysis. *Adv. Mater.* **2019**, *31*(7), 1804672.

89. Wiggins-Camacho, J.D.; Stevenson, K.J. Effect of Nitrogen Concentration on Capacitance, Density of States, Electronic Conductivity, and Morphology of N-Doped Carbon Nanotube Electrodes. *J. Phys. Chem. C* **2009**, *113*(44), 19082.

90. Liu, J.; Gong, Z.; Yan, M.; He, G.; Gong, H.; Ye, G.; Fei, H. Electronic Structure Regulation of Single-Atom Catalysts for Electrochemical Oxygen Reduction to H_2O_2. *Small* **2022**, *18*(3), 2103824.

91. Deng, D.; Yu, L.; Pan, X.; Wang, S.; Chen, X.; Hu, P.; Sun, L.; Bao, X. Size Effect of Graphene on Electrocatalytic Activation of Oxygen. *Chem. Commun.* **2011**, *47*(36), 10016.

92. San Roman, D.; Krishnamurthy, D.; Garg, R.; Hafiz, H.; Lamparski, M.; Nuhfer, N.T.; Meunier, V.; Viswanathan, V.; Cohen-Karni, T. Engineering Three-Dimensional (3D) Out-of-Plane Graphene Edge Sites for Highly Selective Two-Electron Oxygen Reduction Electrocatalysis. *ACS Catal.* **2020**, *10*(3), 1993.

93. Zhang, T.; Li, W.; Huang, K.; Guo, H.; Li, Z.; Fang, Y.; Yadav, R.M.; Shanov, V.; Ajayan, P.M.; Wang, L.; et al. Regulation of Functional Groups on Graphene Quantum Dots Directs Selective CO_2 to CH_4 Conversion. *Nat. Commun.* **2021**, *12*(1), 5265.

94. Song, D.; Guo, H.; Huang, K.; Zhang, H.; Chen, J.; Wang, L.; Lian, C.; Wang, Y. Carboxylated Carbon Quantum Dot-induced Binary Metal–organic Framework Nanosheet Synthesis to Boost the Electrocatalytic Performance. *Mater. Today* **2022**, *54*, 42–51.

95. Wang, W.; Shang, L.; Chang, G.; Yan, C.; Shi, R.; Zhao, Y.; Waterhouse, G.I.N.; Yang, D.; Zhang, T. Intrinsic Carbon-Defect-Driven Electrocatalytic Reduction of Carbon Dioxide. *Adv. Mater.* **2019**, *31*(19), 1808276.

96. Zhu, J.; Huang, Y.; Mei, W.; Zhao, C.; Zhang, C.; Zhang, J.; Amiinu, I.; Mu, S. Effects of Intrinsic Pentagon Defects on Electrochemical Reactivity of Carbon Nanomaterials. *Angew. Chem. Int. Ed.* **2019**, *58*, 3859.

97. Lee, S.; Kim, H.; Lee, J.; Kuk, Y.; Chung, K.H.; Kim, H.; Kahng, S.-J. Donor and Acceptor-like Electronic States in a One-dimensional Semiconductor. *Surf. Sci.* **2006**, *600*(22), 4937.

98. Fan, H.; Wang, J.; Wu, P.; Zheng, L.; Xiang, J.; Liu, H.; Han, B.; Jiang, L. Hydrophobic Ionic Liquid Tuning Hydrophobic Carbon to Superamphiphilicity for Reducing Diffusion Resistance in Liquid-liquid Catalysis Systems. *Chem* **2021**, *7*(7), 1852.

99. Chen, Q.; Peng, Q.; Zhao, X.; Sun, H.; Wang, S.; Zhu, Y.; Liu, Z.; Wang, C.; He, X. Grafting Carbon Nanotubes Densely on Carbon Fibers by Poly (propylene imine) for Interfacial Enhancement of Carbon Fiber Composites. *Carbon* **2020**, *158*, 704–710.

100. Yang, F.; Ma, X.; Cai, W.-B.; Song, P.; Xu, W. Nature of Oxygen-Containing Groups on Carbon for High-Efficiency Electrocatalytic CO_2 Reduction Reaction. *J. Am. Chem. Soc.* **2019**, *141*(51), 20451.

101. Sang, Z.-y.; Hou, F.; Wang, S.-h.; Liang, J. Research Progress on Carbon-based Non-metallic Nanomaterials as Catalysts for the Two-electron Oxygen Reduction for Hydrogen Peroxide Production. *New Carbon Mater* **2022**, *37*(1), 136–151.

102. Yan, H.; Zhao, X.; Guo, N.; Lyu, Z.; Du, Y.; Xi, S.; Guo, R.; Chen, C.; Chen, Z.; Liu, W.; et al. Atomic Engineering of High-density Isolated Co Atoms on Graphene with Proximal-atom Controlled Reaction Selectivity. *Nat. Commun.* **2018**, *9*(1), 3197.

103. Zhou, W.; Xie, L.; Gao, J.; Nazari, R.; Zhao, H.; Meng, X.; Sun, F.; Zhao, G.; Ma, J. Selective H_2O_2 Electrosynthesis by O-doped and Transition-metal-O-doped Carbon Cathodes via O_2 Electroreduction: A Critical Review. *Chem. Eng. J.* **2021**, *410*, 128368.

104. Xie, L.; Zhou, W.; Qu, Z.; Ding, Y.; Gao, J.; Sun, F.; Qin, Y. Understanding the Activity Origin of Oxygen-doped Carbon Materials in Catalyzing the Two-electron Oxygen Reduction Reaction Towards Hydrogen Peroxide Generation. *J. Colloid Interface Sci.* **2022**, *610*, 934–943.

105. Chen, Z.; Chen, S.; Siahrostami, S.; Chakthranont, P.; Hahn, C.; Nordlund, D.; Dimosthenis, S.; Nørskov, J.K.; Bao, Z.; Jaramillo, T.F. Development of a Reactor with Carbon Catalysts for Modular-scale, Low-cost Electrochemical Generation of H_2O_2. *React. Chem. Eng.* **2017**, *2*(2), 239–245.

106. Xia, C.; Xia, Y.; Zhu, P.; Fan, L.; Wang, H. Direct Electrosynthesis of Pure Aqueous H_2O_2 Solutions up to 20% by Weight Using a Solid Electrolyte. *Science* **2019**, *366*(6462), 226.

107. Zhao, J.; Zhang, X.; Xu, J.; Tang, W.; Lin Wang, Z.; Ru Fan, F. Contact-electro-catalysis for Direct Synthesis of H_2O_2 under Ambient Conditions. *Angew. Chem. Int. Ed.* **2023**, *62*(21), e202300604.

108. Zhu, X.; Tan, X.; Wu, K.-H.; Haw, S.-C.; Pao, C.-W.; Su, B.-J.; Jiang, J.; Smith, S.C.; Chen, J.-M.; Amal, R.; et al. Intrinsic ORR Activity Enhancement of Pt Atomic Sites by Engineering the d-Band Center via Local Coordination Tuning. *Angew. Chem. Int. Ed.* **2021**, *60*(40), 21911.

109. Zhang, Q.; Guan, J. Applications of Atomically Dispersed Oxygen Reduction Catalysts in Fuel Cells and Zinc–Air Batteries. *Energy Environ. Mater.* **2021**, *4*(3), 307–335.